

Monosolvation of *R*-1-Phenyl-2,2,2-trifluoroethanol with Amines: Configurational Effects on the Excitation, Ionization, and Fragmentation of Diastereomeric Complexes[†]

Anna Giardini,^{*,‡} Gianfranco Cattenacci,[‡] Alessandra Paladini,[§] Susanna Piccirillo,^{||} Mauro Satta,[⊥] Flaminia Rondino,[#] and Maurizio Speranza[#]

Dipartimento di Chimica and Dipartimento di Studi di Chimica e Tecnologia delle Sostanze Biologicamente Attive, Università di Roma "La Sapienza", P. zle Aldo Moro 5, I-00185 Rome, Italy, CNR, Istituto di Metodologie Inorganiche e dei Plasmi, Sede di Potenza, I-85050, Tito Scalo (PZ) Italy, Università di Roma "Tor Vergata", Via della Ricerca Scientifica, I-00133 Rome, Italy, and CNR, Istituto dei Sistemi Complessi, Sede di Roma, Via dei Taurini 19, I-00185 Rome, Italy

Received: July 27, 2007; In Final Form: September 7, 2007

Wavelength and mass selected resonant two-photon ionization spectra of molecular clusters between *R*-1-phenyl-2,2,2-trifluoroethanol (FE_R) and methylamine (M) or the enantiomers of 2-aminobutane (A_R and A_S) were recorded after supersonic molecular beam expansion and analyzed with the aid of ab initio molecular orbital calculations. The experimental results agree with theoretical calculations pointing to the predominance of the two most stable conformers of monosolvated FE_R whose CF₃ group establishes intense NH⋯F interactions with the selected amines so as to orient them away from the aromatic ring. This reduces the enantioselectivity of FE_R toward the 2-aminobutane enantiomers as compared to that exhibited by the *R*-1-phenylethanol (E_R) analogue, where obviously NH⋯F interactions are absent.

Introduction

Stereochemically defined fluorinated organic compounds are commonly used in bioorganic and medicinal chemistry as antitumor agents and as a probe in studying enzyme activity, reaction mechanisms, and biomolecular binding. The need to explore the physicochemical properties of fluorinated compounds has recently been recognized by researchers who are not in the traditional fluorine chemistry field. From a steric standpoint, fluorine is a good hydrogen mimic. However, it has electronic properties largely different from those of hydrogen. Therefore, replacement of hydrogen atoms by fluorine into organic molecules may cause important physical and chemical changes so as to influence partially or even control completely the stereochemical outcome of reactions.^{1–3} Fluorine may act as a weak hydrogen bond acceptor, and therefore, a fluorinated molecule may establish noncovalent interactions that are absent with its nonfluorinated analogue.⁴

In recent years, considerable progress has been made in the detailed study of weakly bonded molecular complexes between chiral molecules in the gas phase to understand molecular interactions at the most basic molecular level, crucial to characterize the principles that govern chiral recognition.^{5,15} Resonant two-photon ionization (R2PI) spectroscopy, coupled with time-of-flight (TOF) mass spectrometry, on cooled complexes in a supersonic beam were revealed as an excellent tool for investigating the structure and specific intermolecular interactions in hydrogen bonded clusters between chiral aromatic

alcohols and a variety of solvent molecules, including chiral mono- and bifunctional alcohols, amines, and water. The results of these gas phase studies are particularly useful since they refer to an isolated system unperturbed by environmental effects and, therefore, directly comparable to theoretical predictions.^{10,14} Very recently, we applied this methodology to the study of *R*-1-phenyl-2,2,2-trifluoroethanol (FE_R) and its cluster with water¹⁶ and compared the results with those obtained for the nonfluorinated analogue *R*-1-phenylethanol (E_R). We showed that the most stable conformer of FE_R exhibits an intramolecular hydrogen bond between the OH group and one of the fluorine atoms of a -CF₃ group, differently from the analogous E_R molecule, where an OH⋯π hydrogen bond interaction is present.¹⁷ In the monohydrated cluster [FE_R·H₂O], the water molecule acts as a proton acceptor from the hydroxyl group of FE_R and as a proton donor to the fluorine atom. In the [E_R·H₂O] cluster, the water molecule acts as a proton acceptor from the OH group of the chromophore and as a proton donor toward its π ring. In this context, it appears of some interest to extend the investigation to FE_R complexes with more basic solvent molecules, such as methylamine (M) and the *R*- and *S*-enantiomers of 2-aminobutane (A_R and A_S, respectively). This study allows us to explore, through R2PI spectroscopy, the role of N–H⋯F and OH⋯N and dispersive interactions in the chiral recognition of FE_R toward the amines and to compare the results with those obtained for the analogous clusters involving the nonfluorinated chromophore E_R.

Experimental Procedures

The experimental R2PI-TOF setup has been described elsewhere.¹⁸ The supersonic beam of the species of interest was obtained by adiabatic expansion of a carrier gas (Ar; stagnation pressure from 2 to 4 bar), seeded with *R*-1-phenyl-2,2,2-trifluoroethanol (FE_R; Aldrich 99%) and the selected amine (Aldrich ≥98%) through a heated pulsed nozzle of an 800 μm

[†] Part of the "Giacinto Scoles Festschrift".

* Corresponding author. Tel.: +39-06-49913358; fax: +39-06-490324; e-mail: anna.giardini@uniroma1.it.

[‡] Dipartimento di Chimica, Università di Roma "La Sapienza".

[§] Consiglio Nazionale delle Ricerche IMIP.

^{||} Università di Roma 2 "Tor Vergata".

[⊥] Consiglio Nazionale delle Ricerche ISC.

[#] Dipartimento di Studi di Chimica e Tecnologia delle Sostanze Biologicamente Attive, Università di Roma "La Sapienza".

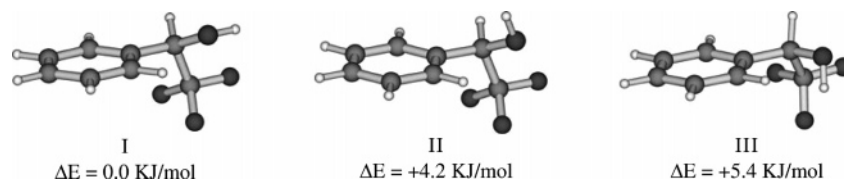


Figure 1. MP2/6-31G (d,p)-optimized structures and relative energies of the three most stable minima on the FE_R PES.

i.d. nozzle (aperture time: 200 μ s; repetition rate: 10 Hz) heated at $T = 80$ °C. The concentration of the trace components was maintained low enough to minimize the production of heavier clusters. The molecular beam was allowed to pass through a 1 mm diameter skimmer into a second chamber equipped with a TOF spectrometer oriented perpendicular to the supersonic beam direction. Molecules and clusters in the beam were excited and ionized by a tunable dye laser, pumped by a Nd:YAG laser ($\lambda = 532$ nm). The dye fundamental frequencies were doubled and, when necessary, mixed with residual 1064 nm radiation. The ions formed by R2PI ionizations were mass discriminated and detected by a channeltron after a 50 cm flight path. The mass selected ionic signals were recorded and averaged by a digital oscilloscope and stored in a PC. One-color R2PI experiments (1cR2PI) involve electronic excitation of the species of interest by absorption of one photon $h\nu_1$ and by its ionization by a second photon of the same energy $h\nu_1$. The 1cR2PI excitation spectra were obtained by recording the entire TOF mass spectrum as a function of ν_1 . The wavelength dependence of a given mass resolved ion represents the absorption spectrum of the species and contains important information about its electronic excited state S_1 .

Computational Details

MM3 force-field classical molecular dynamics is run just as a starting point for each neutral adduct at a temperature of 800 K with some constraints to overcome dissociation; the cumulative time is 0.1 ns with a time step of 0.5 fs and a dump time of 1 ps. The 100 snapshots are then optimized with a convergence of 4×10^{-6} kJ mol $^{-1}$ /Å rms gradient per atom. Initially, the obtained optimized structures are classified according to their energy and conformation. The chromophore has then been reoptimized at the MP2/6-31G** level of theory, and the amine clusters have been studied by a DFT approach: we used, due to computational time constraints, only the B3LYP Hamiltonian with the 6-31G** basis set for both energy and geometrical optimization. All the ab initio calculations were performed using the Gaussian 98 package.¹⁹ Vibrational frequencies were calculated using the B3LYP density functional method and a 6-31G** basis set, previously found to give fair agreement with experimental data for similar molecules when scaling factors of 0.97 are used. The spectral $\pi^* \leftarrow \pi$ electronic transitions of the bare FE_R have been calculated through ab initio CASSCF studies, with Pople and Slater-type Gaussian basis sets.²⁰

Results and Discussion

FE_R Molecule. The most stable conformations of the FE_R molecule, previously reported,¹⁶ are summarized here. Three local minima are identified on the HF/6-31G** calculated potential energy surface (PES). Their MP2/6-31G (d,p) calculated structures and relative energies are illustrated in Figure 1. The most stable conformer I is characterized by an OH group, located out of the plane of the phenyl ring and H-bonded to the fluorine atom of the CF_3 group oriented anti to the ring plane. No $OH \cdots F$ interactions are present in the 4.2 kJ mol $^{-1}$ less stable

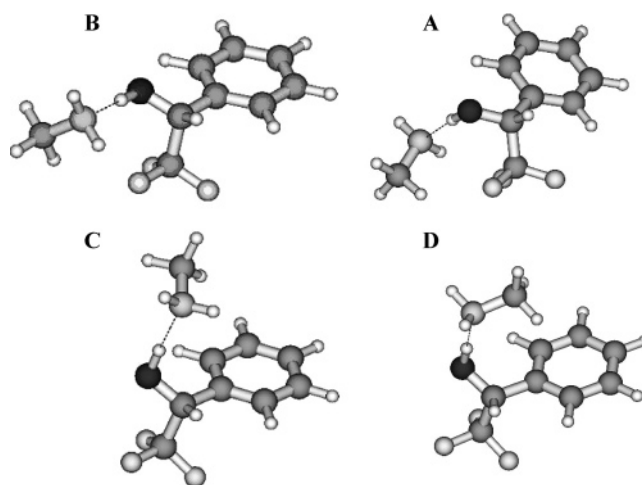


Figure 2. Ab initio B3LYP/6-31G** calculated structures of the complex of *R*-1-phenyl-2,2,2-trifluoroethanol with monomethylamine.

conformer II since here the OH hydrogen points toward the ring plane away from all the F atoms. The least stable conformer III differs from I for the $OH \cdots F$ bonding between the OH hydrogen and one of the F atoms oriented gauche to the phenyl ring. According to the MP2/6-31G (d,p) relative stability of I–III and the potential energy barriers for the I \rightarrow II (9.6 kJ mol $^{-1}$) and II \rightarrow III (3.5 kJ mol $^{-1}$) conversions, conformer I is expected to predominate in the supersonic expansion of FE_R . The excitation spectrum of FE_R is characterized by a very intense band at 37782 cm $^{-1}$, assigned to the $S_1 \leftarrow S_0$ electronic excitation of the most stable conformer I on the basis of theoretical predictions.^{19,20} Other intense vibronic bands toward the blue are attributed to its vibronic transitions.¹⁷

[$FE_R \cdot M$] Complex. Ab initio calculations were performed for monosolvated [$FE_R \cdot M$] clusters of the low lying monomer structures. As a starting point, initial structures were constructed by placing the M molecule around the principal interaction sites of FE_R : the hydroxyl group, the fluorine atoms, and the π system of the aromatic ring. Full ab initio optimization of the obtained structures resulted in four lowest energy conformers A–D differing in the specific interactions of the chromophore with the solvent molecule (Figure 2). The relevant geometrical parameters are listed in Table 1 together with the relative energies corrected for the zero-point energy differences and BSSE.

One color mass selected R2PI spectra of a mixture of FE_R and M seeded in argon, recorded in the mass channels $m/z = 207$ ($[FE_R \cdot M]^+$), 138 ($[(FE_R \cdot CF_3) \cdot M]^+$), and 32 ($[MH]^+$), are shown in Figure 3a–c, respectively. The spectra are characterized by two intense bands at 37 783 cm $^{-1}$ (α) and at 37 771 cm $^{-1}$ (β). Band α of Figure 3 almost coincides with the 0 $_0^0$ band origin of bare FE_R ($\Delta\nu = +1$ cm $^{-1}$), while the other is red-shifted by -11 cm $^{-1}$ (Table 2). In the fragment mass channels $[MH]^+$ and $[(FE_R \cdot CF_3) \cdot M]^+$, band α is characterized by a stronger intensity with respect to β . On this basis, the two bands can be tentatively assigned to the 0 $_0^0$ electronic transition $S_1 \leftarrow S_0$ of two distinct singly solvated [$FE_R \cdot M$] conformers.

TABLE 1: B3LYP/6-31G Optimized Structural Parameters and Relativities Energies Corrected for the Zero-Point Energy Differences and BSSE of Complexes between FE_R with Monomethylamine (M) and Buthylamine (A_RS)**

system	calcd structure	<i>E</i> (kJ/mol)	$\alpha(\text{C}_\beta\text{C}_\alpha-\text{C}_1\text{C}_2)$	$\beta(\text{OC}_\alpha-\text{C}_1\text{C}_2)$	$\gamma(\text{OH}-\text{C}_\alpha\text{C}_1)$	$\delta(\text{OH}-\text{C}_\alpha\text{C}_\beta)$	$\epsilon(\text{FC}_\beta-\text{C}_\alpha\text{C}_1)$	$R(\text{\AA})_{\text{C}_2\cdots\text{H}(\text{O})}$	$R(\text{\AA})_{\text{N}\cdots\text{H}(\text{O})}$	$R(\text{\AA})_{\text{F}\cdots\text{H}(\text{N})}$
[FE _R M]	A	+1.63	129.0	2.7	68.6	301.3	308.1 (gauche)	2.82	1.78	2.46
	B	0.00	99.8	338.1	194.6	72.4	179.8 (anti)	3.74	1.78	2.65
	C	+6.07	88.5	328.6	294.9	172.3		3.02	1.81	
	D	+6.82	88.6	328.6	290.3	167.8		3.08	1.82	
[FE _R AR]	A _{homo}	+0.06	123.4	357.9	70.0	302.8	303.2 (gauche)	2.82	1.78	2.54
	B _{homo}	0.00	97.8	335.9	188.2	65.9	177.8 (anti)	3.75	1.78	2.49
	C _{homo}	+1.64	88.5	328.6	291.3	168.7		3.07	1.80	
	D _{homo}	+2.25	93.3	333.3	275.8	153.2		3.23	1.82	
[FE _R AS]	A _{hetero}	+3.18	122.2	356.2	74.1	307.2	305.4 (gauche)	2.87	1.78	2.75
	B _{hetero}	0.00	94.5	332.4	181.3	59.0	174.3 (anti)	3.75	1.78	2.55
	C _{hetero}	+7.66	88.4	328.6	296.5	174.0		3.00	1.80	
	D _{hetero}	+10.36	95.0	334.6	269.4	146.5		3.29	1.81	

Detailed analysis of the structural features of the most stable calculated isomers A and B (Figure 2 and Table 1) allows us to identify them as responsible for the intense bands at $\Delta\nu = +1$ and -11 cm^{-1} in Figure 3. In fact, the limited spectral shifts of these bands are consistent with the dual function of the NH₂ group of the amine both as a H-bond acceptor from the OH of FE_R ($R_{\text{N}\cdots\text{H}(\text{O})} = 1.78 \text{ \AA}$) and as H-bond donor to one of its F atoms ($R_{\text{F}\cdots\text{H}(\text{N})} = 2.46, 2.65 \text{ \AA}$). This dual function, as well as the limited dispersive interactions between the FE_R aromatic ring and the distant amine, suggests that the π electron densities of the ground state and excited FE_R are only slightly perturbed by the presence of the M molecule.

The assignment of each of the α and β bands to conformers A and B is supported by the analysis of the 1cR2PI-TOF mass spectra of [FE_R·M], recorded at $\nu = 37783 \text{ cm}^{-1}$ (band α) and $\nu = 37771 \text{ cm}^{-1}$ (band β) (Figure 4). The major difference

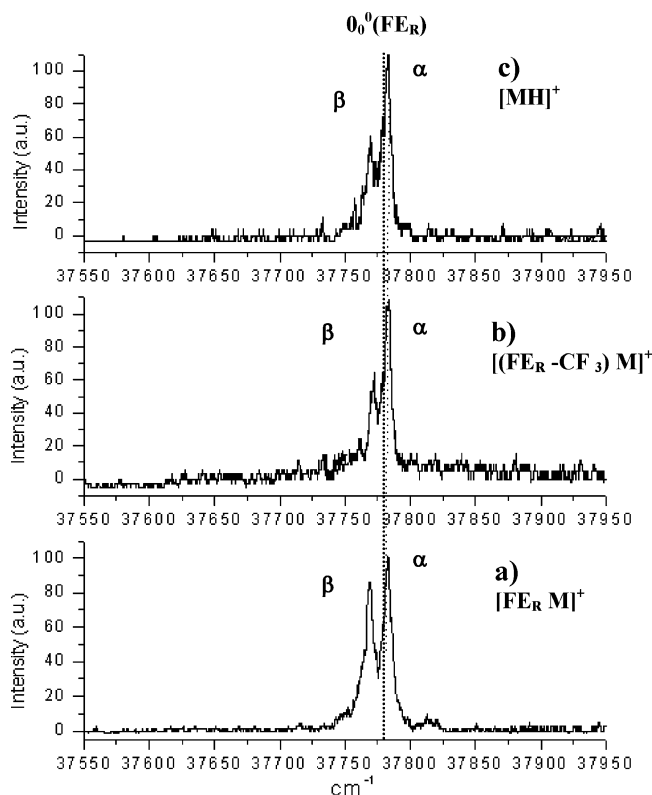


Figure 3. 1cR2PI excitation spectra of the complex of *R*-1-phenyl-2,2,2-trifluoroethanol (FE_R) with methylamine (M) obtained by monitoring the ion signal (a) at the complex mass [FE_R·M]⁺ (m/z 207); (b) at the ethyl loss fragment mass [(FE_R-CF₃)·M]⁺ (m/z 138); and (c) at the protonated amine fragment mass [MH]⁺ (m/z 32). The dotted line refers to the 0₀⁰ transition for the most stable conformer I of the bare chromophore FE_R.

TABLE 2: Band Shifts ($\Delta\nu$) of Supersonically Expanded 1:1 Complexes between FE_R and Monomethylamine (M) and Buthylamine (A) Relative to the S₁ ← S₀ Electronic Band Origin of the Bare Chromophore FE_R

cluster	band	$\nu (\text{cm}^{-1})$	$\Delta\nu (\text{cm}^{-1})$
[FE _R M]	a	37 783	+1
	b	37 771	-11
	g	37 757	-25
	d	37 733	-49
[FE _R AR]	α_R	37 777	-5
	β_R	37 755	-27
	γ_R	37 645	-137
	δ_R	37 599	-183
[FE _R AS]	α_S	37 779	-3
	β_S	37 757	-25
	γ_S	37 628	-154
	δ_S	37 612	-170

between the two spectra concerns the much extensive [FE_R·M]⁺ → [(FE_R-CF₃)·M]⁺ + ·CF₃ fragmentation in the mass spectrum in resonance with band α relative to that taken in resonance with band β . This observation can be rationalized with the aid of the B3LYP/6-31G** calculated potential energy profiles for the fragmentation of [FE_R·M]⁺ (Figure 5). The calculations reveal that two-photon ionization of [FE_R·M] leads to a common [FE_R·M]⁺ ion structure, irrespective of that of its neutral precursor, whether A or B. This means that the overall activation energy difference for the A → A⁺ → [(FE_R-CF₃)·M]⁺ + ·CF₃ and B → B⁺ → [(FE_R-CF₃)·M]⁺ + ·CF₃ sequences reflects essentially the stability gap between the A and the B

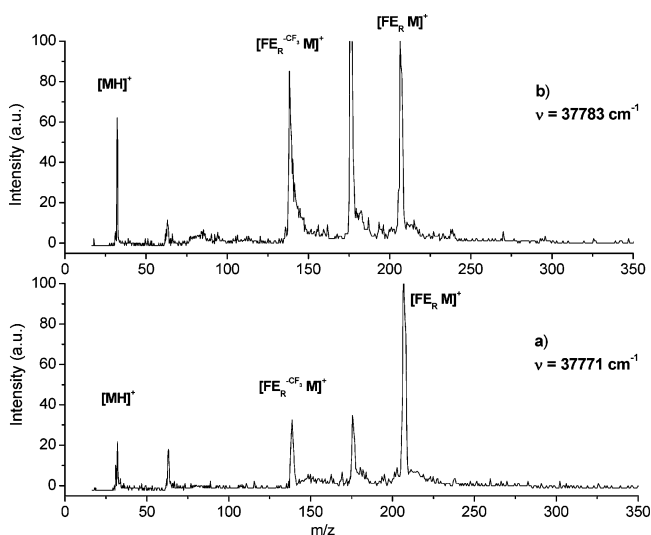


Figure 4. Time-of-flight mass spectra of a *R*-1-phenyl-2,2,2-trifluoroethanol and monomethylamine mixture measured and recorded at $\nu = 37783 \text{ cm}^{-1}$ (a) and $\nu = 37771 \text{ cm}^{-1}$ (b).

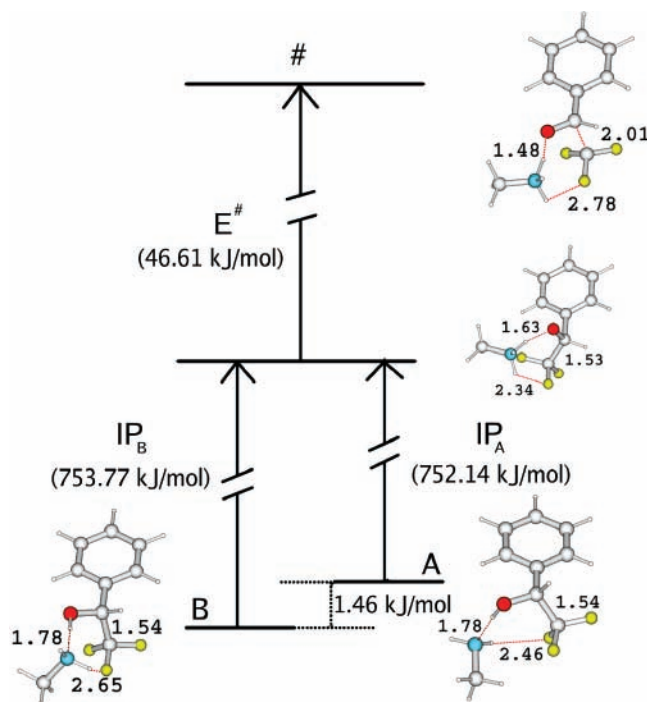


Figure 5. Structures of neutral A and B conformers of $[\text{FE}_R \cdot \text{M}]$, of their common $[\text{FE}_R \cdot \text{M}]^+$ ion, and of the transition state for the $[\text{FE}_R \cdot \text{M}]^+ \rightarrow [\text{FE}_R\text{-CF}_3] \cdot \text{M}^+ + \cdot \text{CF}_3$ fragmentation.

conformers in their ground state. It follows that the 1.63 kJ mol^{-1} more stable B isomer is expected to undergo less extensive fragmentation than the less stable A conformer. In agreement with the mass spectra of Figure 4, the band β is assigned to conformer B and the band α to isomer A.

The intensity of other bands present in the excitation spectrum of Figure 2 is almost negligible, suggesting the hypothesis that the population of the less stable C and D isomers (Table 2) of the $[\text{FE}_R \cdot \text{M}]$ cluster is not appreciable.

Diastereomeric $[\text{FE}_R \cdot \text{A}]$ Complexes. The 1cR2PI excitation spectra of the homochiral $[\text{FE}_R \cdot \text{A}_R]$ and the heterochiral $[\text{FE}_R \cdot \text{A}_S]$ complexes, taken at $m/z = 249$ ($[\text{FE}_R \cdot \text{A}]^+$), are shown in Figure 6a,b, respectively. Identical spectra have been recorded in the fragmentation channels at m/z 180 ($[(\text{FE}_R\text{-CF}_3) \cdot \text{A}]^+$) and 74 ($[\text{AH}]^+$). The spectrum of the homochiral $[\text{FE}_R \cdot \text{A}_R]$ complex is characterized by a very intense band at $37\,755 \text{ cm}^{-1}$ (β_R) accompanied by a less intense band at $37\,777 \text{ cm}^{-1}$ (α_R) and by two small red-shifted bands, at $37\,645 \text{ cm}^{-1}$ (δ_R) and $37\,599 \text{ cm}^{-1}$ (γ_R). Analogously, the spectrum of the heterochiral $[\text{FE}_R \cdot \text{A}_S]$ complex exhibits a very intense signal at $37\,757 \text{ cm}^{-1}$ (β_S), accompanied by a less intense band at $37\,779 \text{ cm}^{-1}$ (α_S) and by two small bands at $37\,628 \text{ cm}^{-1}$ (δ_S) and $37\,612 \text{ cm}^{-1}$ (γ_S). The same pattern is found around $38\,200 \text{ cm}^{-1}$ and corresponds to a intense butterfly vibronic transition of the cluster. This suggests the assignment of bands α_R , β_R , δ_R , γ_R and α_S , β_S , δ_S , γ_S to the $0_0^0 S_1 \leftarrow S_0$ electronic transition of four distinct $[\text{FE}_R \cdot \text{A}_R]$ and $[\text{FE}_R \cdot \text{A}_S]$ isomers. The values of the shifts with respect to the $0_0^0 S_1 \leftarrow S_0$ electronic transition of the bare chromophore are reported in Table 2.

The B3LYP/6-31G** calculated potential energy surfaces of the diastereomeric $[\text{FE}_R \cdot \text{A}_R]$ and $[\text{FE}_R \cdot \text{A}_S]$ complexes reveal the presence of four lowest energy critical structures differing in the conformation of the chromophore and in the specific interaction with the solvent (Figure 7). The relevant geometrical parameters are listed in Table 1 together with their relative energies. Analysis of Table 1 indicates that the most stable isomers A and B of $[\text{FE}_R \cdot \text{M}]$ are structurally similar to

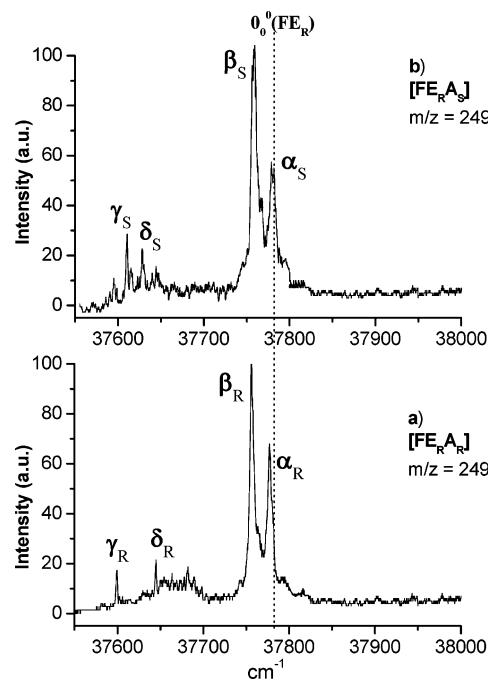


Figure 6. 1cR2PI excitation spectra of the complexes between FE_R with (a) A_R and (b) A_S . The dotted line refers to the 0_0^0 transition for the most stable conformer I of the bare chromophore FE_R .

conformers A_{hetero} and B_{hetero} of $[\text{FE}_R \cdot \text{A}_S]$ and to conformers A_{homo} and B_{homo} of $[\text{FE}_R \cdot \text{A}_R]$. The $\text{A} < \text{B}$ stability order for $[\text{FE}_R \cdot \text{M}]$ ($\Delta E = E_A - E_B = +1.63 \text{ kJ mol}^{-1}$) is maintained for $[\text{FE}_R \cdot \text{A}_S]$ ($\text{A}_{\text{hetero}} < \text{B}_{\text{hetero}}$; $\Delta E = +3.18 \text{ kJ mol}^{-1}$), whereas the two forms are virtually degenerate in $[\text{FE}_R \cdot \text{A}_R]$ ($\text{A}_{\text{homo}} \approx \text{B}_{\text{homo}}$; $\Delta E = -0.25 \text{ kJ mol}^{-1}$). Following the same line of reasoning used for $[\text{FE}_R \cdot \text{M}]$, the most stable conformers of the homo- and heterochiral $[\text{FE}_R \cdot \text{A}_R]$ and $[\text{FE}_R \cdot \text{A}_S]$ clusters should display the 1cR2PI-TOF mass spectrum with the lowest fragmentation pattern. Accordingly (see Figure S2 in the Supporting Information), the most intense signal at $\nu = 37\,757 \text{ cm}^{-1}$ (β_S) of Figure 6b is associated with structure B_{hetero} of $[\text{FE}_R \cdot \text{A}_S]$, while the less intense peak at $\nu = 37\,779 \text{ cm}^{-1}$ (α_S) is attributed to the A_{hetero} isomer. By analogy (see Figure S1 in the Supporting Information), the most intense band at $\Delta\nu = 37\,755 \text{ cm}^{-1}$ (β_R) of Figure 6a is assigned to isomer B_{homo} of $[\text{FE}_R \cdot \text{A}_R]$, while the less intense band at $\nu = 37\,777 \text{ cm}^{-1}$ (α_R) is attributed to the A_{homo} structure.

Assignment of the small red-shifted bands δ_R and γ_R in Figure 6a and at δ_S and γ_S in Figure 6b requires a comparative analysis of the structural features of the less stable $\text{C}_{\text{homo}}/\text{D}_{\text{homo}}$ and $\text{C}_{\text{hetero}}/\text{D}_{\text{hetero}}$ pairs. Thus, the structure of the least stable D_{homo} and D_{hetero} isomers is characterized by the amine H-bonded to the OH group of FE_R ($R_{\text{N} \cdots \text{H}(\text{O})} = 1.82, 1.81 \text{ \AA}$) and by the 2-butyl group lying over the aromatic ring of the chromophore. In this way, the amine establishes effective dispersive interactions with the π system of the chromophore. Similar interactions are less pronounced in the slightly more stable C_{homo} and C_{hetero} structures. On these grounds, one should expect that the band origins of D_{homo} and D_{hetero} are more red-shifted than those of C_{homo} and C_{hetero} , respectively. Therefore, the $37\,645 \text{ cm}^{-1}$ band of Figure 6a is attributed to isomer C_{homo} and the $37\,599 \text{ cm}^{-1}$ band to conformer D_{homo} . In the same fashion, the $37\,628 \text{ cm}^{-1}$ and $37\,612 \text{ cm}^{-1}$ signals of Figure 6b are assigned to isomers C_{hetero} and D_{hetero} , respectively.

As pointed out previously, the CF_3 group of FE_R forms with the selected amines an intense $\text{NH} \cdots \text{F}$ interaction, which orients the amines away from the aromatic ring. This reduces the R2PI

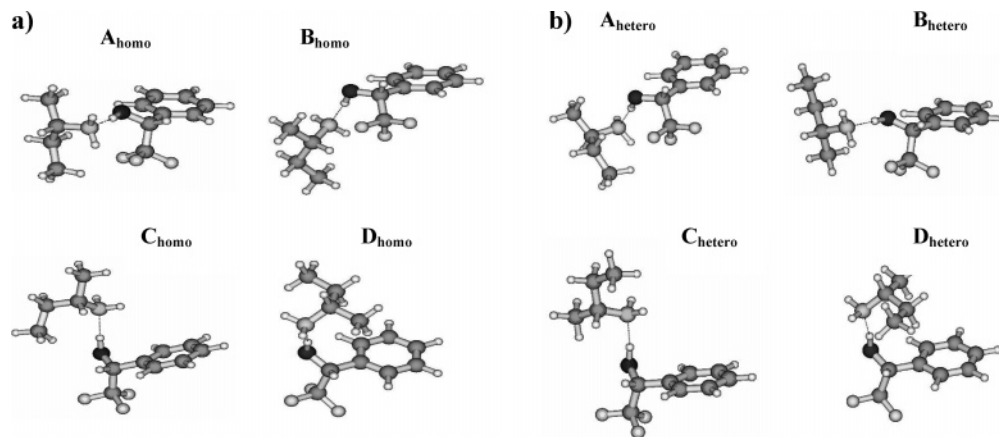


Figure 7. Ab initio B3LYP/6-31G** calculated structures of the complex of FE_R with (a) A_R and (b) A_S .

enantioselectivity of FE_R as compared to that of E_R , where any intracomplex $NH\cdots F$ bonding is obviously absent. A variety of chiral solvent molecules, including A_R and A_S , can establish effective dispersive interactions with the π system of E_R , whose magnitude depends on the configuration of the solvent molecule. This results in a large, easily measurable difference of the spectral shifts of diastereomeric complexes of A_R and A_S with E_R (e.g., $\Delta\Delta\nu = \Delta\nu_{\text{homo}} - \Delta\nu_{\text{hetero}} = +17 \text{ cm}^{-1}$ for $[E_R\cdot A_R]$ and $[E_R\cdot A_S]$).¹³ No such pronounced differences have been measured for the most stable conformers of the $[FE_R\cdot A_R]$ and $[FE_R\cdot A_S]$ complexes ($\Delta\Delta\nu = \Delta\nu(A_{\text{homo}}) - \Delta\nu(A_{\text{hetero}}) = \Delta\nu(B_{\text{homo}}) - \Delta\nu(B_{\text{hetero}}) = -2 \text{ cm}^{-1}$; Table 2). Instead, $\Delta\Delta\nu$ values, approaching those of $[E_R\cdot A_R]$ and $[E_R\cdot A_S]$, are measured for the $D_{\text{homo}}/D_{\text{hetero}}$ ($\Delta\Delta\nu = -13 \text{ cm}^{-1}$) and $C_{\text{homo}}/C_{\text{hetero}}$ ($\Delta\Delta\nu = +17 \text{ cm}^{-1}$) diastereomeric pairs. This similarity is not fortuitous since the $D_{\text{homo}}/C_{\text{homo}}$ and $D_{\text{hetero}}/C_{\text{hetero}}$ pairs are the only among the $[FE_R\cdot A_R]$ and $[FE_R\cdot A_S]$ conformers wherein the amine moiety may somehow interact with the aromatic ring of the chromophore, much like in the $[E_R\cdot A_R]$ and $[E_R\cdot A_S]$ complexes.

Conclusion

The present study shows how the R2PI spectroscopy, coupled with ab initio calculations, can provide valuable information on the molecular structure of noncovalent complexes and on the interactive forces holding their components together in the unsolvated state. Supersonic expansion of FE_R/M mixtures leads to the formation of two predominant monosolvated $[FE_R\cdot M]$ isomers. Their structural assignment has been based on the spectral shifts of their $S_1 \leftarrow S_0$ electronic band origin relative to that of the bare FE_R as well as on their 1cR2PI-TOF mass spectra, recorded at each $S_1 \leftarrow S_0$ resonance. Accordingly, the two bands, observed in the excitation spectra of $[FE_R\cdot M]$, have been attributed to the isomeric structures A and B characterized by the dual function of the NH_2 group of amine both as H-bond acceptor from the OH group of FE_R and as H-bond donor toward its F atom and by the large distance of the amine from the aromatic ring of the chromophore. Similar structures are responsible of the two major bands, observed in the excitation spectra of the diastereomeric $[FE_R\cdot A_R]$ and $[FE_R\cdot A_S]$ complexes. Two minor, although more red-shifted, bands in the same spectra are attributed to two different structures, both characterized by an $OH\cdots N$ hydrogen bond. In these structures, the amine moiety interacts with the aromatic ring of the chromophore.

In the most stable A_{homo} , B_{homo} , A_{hetero} , and B_{hetero} conformers, the CF_3 group of FE_R establishes an intense $NH\cdots F$ interaction, which pushes the amine away from the aromatic ring. The measured spectral shift difference is very small, 2 cm^{-1} .

Appreciable differences in the spectral shifts of the diastereomeric $[FE_R\cdot A_R]$ and $[FE_R\cdot A_S]$ complexes are indeed observed for the less stable $C_{\text{homo}}/D_{\text{homo}}$ and $C_{\text{hetero}}/D_{\text{hetero}}$ conformers, in particular as regards to the more red-shifted signals ($\Delta\Delta\nu = \Delta\nu_{\text{homo}} - \Delta\nu_{\text{hetero}} = -17$ and $+13 \text{ cm}^{-1}$). These spectral differences reflect essentially the strength of noncovalent forces ($N\cdots H\cdots F$, $OH\cdots N$, and $OH\cdots\pi$ bonds and dispersive interactions) holding together the amine enantiomers and the chiral FE_R chromophore.

Acknowledgment. Contract grant sponsors: Ministero della Università e della Ricerca Scientifica e Tecnologica (MURST-COFIN), Consiglio Nazionale delle Ricerche (CNR), and ASI (Contract Grant NI/015070).

Supporting Information Available: TOF mass spectra. This material is available free of charge via the Internet at <http://pubs.acs.org>.

References and Notes

- (1) Kirk, K. L. *J. Fluorine Chem.* **2006**, *127*, 1013.
- (2) Isanbor, C.; O'Hagan, D. *J. Fluorine Chem.* **2006**, *127*, 303.
- (3) Bégulé, J.-P.; Bonnet-Delpon, D. *J. Fluorine Chem.* **2006**, *127*, 992.
- (4) Vaupel, S.; Brutschy, B.; Tarakeshwar, P.; Kim, K. S. *J. Am. Chem. Soc.* **2006**, *128*, 5417.
- (5) Su, Z.; Borho, N. N.; Xu, Y. *J. Am. Chem. Soc.* **2006**, *128*, 17126.
- (6) Le Barbu-Debus, K.; Lahmani, F.; Zehnacker-Rentien, A.; Guchhait, N.; Panja, S. S.; Chakraborty, Y. *J. Chem. Phys.* **2006**, *125*, 174305-1.
- (7) Le Barbu-Debus, K.; Lahmani, F.; Zehnacker-Rentien, A.; Guchhait, N. *Chem. Phys. Lett.* **2006**, *422*, 218.
- (8) Seurre, N.; Le Barbu-Debus, K.; Lahmani, F.; Zehnacker-Rentien, A.; Borho, N.; Suhm, M. A. *Phys. Chem. Chem. Phys.* **2006**, *8*, 1007.
- (9) Le Barbu-Debus, K.; Lahmani, F.; Zehnacker-Rentien, A.; Guchhait, N. *Phys. Chem. Chem. Phys.* **2006**, *8*, 1001.
- (10) Adler, T. B.; Borho, N.; Reiher, M.; Suhm, M. A. *Angew. Chem., Int. Ed.* **2006**, *45*, 3440.
- (11) Seurre, N.; Le Barbu-Debus, K.; Lahmani, F.; Borho, N.; Suhm, M. A.; Zehnacker, A. *Aust. J. Chem.* **2004**, *57*, 1149.
- (12) Borho, N.; Suhm, M. A. *Org. Biomol. Chem.* **2003**, *1*, 4351.
- (13) Filippi, A.; Giardini, A.; Latini, A.; Piccirillo, S.; Scuderi, D.; Speranza, M. *Int. J. Mass Spectrom.* **2001**, *210–211*, 483.
- (14) Speranza, M.; Satta, M.; Piccirillo, S.; Rondino, F.; Paladini, A.; Giardini, A.; Filippi, A.; Catone, D. *Mass Spectrom. Rev.* **2005**, *24*, 588.
- (15) Le Barbu-Debus, K.; Zehnacker-Rentien, A.; Lahmani, F.; Mons, M.; Piuze, F.; Dimicoli, I. *Chirality* **2001**, *13*, 715.
- (16) Giardini, A.; Rondino, F.; Cattenacci, G.; Paladini, A.; Piccirillo, S.; Satta, M.; Speranza, M. *Chem. Phys. Lett.* **2007**, *435*, 230.
- (17) Giardini Guidoni, A.; Piccirillo, S.; Scuderi, D.; Satta, M.; Di Palma, T. M.; Speranza, M. *Phys. Chem. Phys.* **2000**, *2*, 4139.
- (18) Consalvo, D.; van der Avoird, A.; Piccirillo, S.; Coreno, M.; Giardini Guidoni, A.; Mele, A.; Snels, M. *J. Chem. Phys.* **1993**, *99*, 8398.
- (19) Frisch, M. J.; Trucks, G. W.; Schlegel, H. B.; Scuseria, G. E.; Robb, M. A.; Cheeseman, J. R.; Zakrzewski, V. G.; Montgomery, J. A., Jr.; et al. *Gaussian 98*, revision A.6; Gaussian, Inc.: Pittsburgh, PA, 1998.
- (20) Satta, M.; Sanna, N.; Giardini, A.; Speranza, M. *J. Chem. Phys.* **2006**, *125*, 94101.